

San Jose State University

From the Selected Works of Alejandro Garcia

1986

Nonequilibrium Fluctuations studied by a Rarefied Gas Simulation

Alejandro Garcia, *San Jose State University*

Nonequilibrium fluctuations studied by a rarefied-gas simulation

Alejandro L. Garcia

*Service de Chimie Physique II, Université Libre de Bruxelles, Campus Plaine, Boulevard du Triomphe,
Code Postal No. 231, B-1050 Bruxelles, Belgium*

(Received 2 December 1985)

A dilute gas under a constant heat flux is studied with use of a Monte Carlo simulation based on the Boltzmann equation. Results for several spatial correlation functions of equal-time fluctuations are reported and compared qualitatively with previous fluctuating hydrodynamics calculations for liquids.

The study of thermodynamic fluctuations has in recent years been extended to nonequilibrium systems. One scenario which has been extensively studied by a wide range of methods is that of a fluid subjected to a constant heat flux.¹ Most analytic results to date have been restricted to liquids since (a) the light scattering experiments are most easily performed with liquids and (b) if one assumes that the fluid has a vanishing thermal expansivity then the acoustic and thermal diffusion modes decouple, considerably simplifying the analysis.^{1(b)} Thus, for a liquid, the nonequilibrium modifications to the density-density fluctuation time correlation function are directly observable by light scattering experiments.² Unfortunately, many predictions (such as subtle changes in line shapes) are impossible to confirm given the existing experimental limitations. A natural alternative is to use numerical simulations.³ Though it is possible to simulate a liquid by molecular dynamics, for a number of reasons it is more convenient to study a gas. In this paper, we present some preliminary results of long-ranged nonequilibrium correlation functions observed in a dilute-gas simulation.

There are some differences between the results from a light scattering experiment and those from a numerical simulation. The most important differences arise from the fact that numerical simulations deal with mesoscopic systems (hundreds to thousands of particles) while physical experiments deal with truly macroscopic systems. For example, if we simulate a closed system, the conservation of particle number considerably modifies the correlation functions, as we shall see. Furthermore, the effects of the boundaries are extremely important in these simulations. One common feature among experiments and simulations: nonequilibrium effects are subtle and require long observations times. For simulations this translates to many hours of computer time.

With the limitations of our computer facilities in mind we chose to employ a dilute-gas simulation based on the Boltzmann equation rather than attempting a molecular-dynamics approach. Such simulations have been used successfully by Bird and others in rarefied-gas dynamics.⁴ As both the theoretical foundations and the details of implementation are nicely discussed by Bird, we only give a brief sketch of the method. The state of the system is stored as the positions and velocities of all the particles.

The evolution of the system is integrated in time steps which are a small fraction of the mean collision time. During a time step, the free-flight motion and collisional motion are considered to be decoupled. As such, all the particles are first moved and then a set of representative collisions are computed among the set of candidate collision partners. These simulations are considerably faster than molecular dynamics because the exact positions of the particles are not employed in the computation of collisions, instead all particles within a volume element are candidate collision partners. Collision partners are accepted or rejected on the basis of their relative speed. The Monte Carlo selection of collision times assumes a Maxwell-Boltzmann distribution within the volume element. This local equilibrium assumption is entirely within the spirit of fluctuating hydrodynamics.

The system we studied contained 2000 hard-sphere particles between two stationary plates at temperatures T_1 and T_2 , separated by a distance L . The interplate distance was chosen such that at equilibrium the distance was equal to ten mean-free paths. Runs were made for temperature gradients of $T_1 = 1$, $T_2 = 1, 3$, and 5 . A single run was made for an equilibrium system in the presence of a gravitational field; for this run there was a density gradient but no temperature gradient. In each case, the system was initialized near the steady state and evolved for about 10^6 collisions before beginning the accumulation of statistics as it has been found that the initial conditions can severely contaminate the statistics.⁵ For the computation of the spatial correlation functions the system was divided into 20 cells. In Figs. 1 and 2 we plot the density and temperature gradients for the various cases studied.

In this work we report on three spatial correlation functions of equal-time fluctuations which have been of theoretical interest. First, consider the (number) density-density correlation function, which at equilibrium is of the form

$$\langle \delta n_i \delta n_j \rangle = n_i \delta_{ij}^{Kr} - \frac{n_i n_j}{\sum_{k=1}^M n_k}, \quad i, j = 1, 2, \dots, M \quad (1)$$

where n_i is the average number density of cell i . The second term arises from the conservation of particle num-

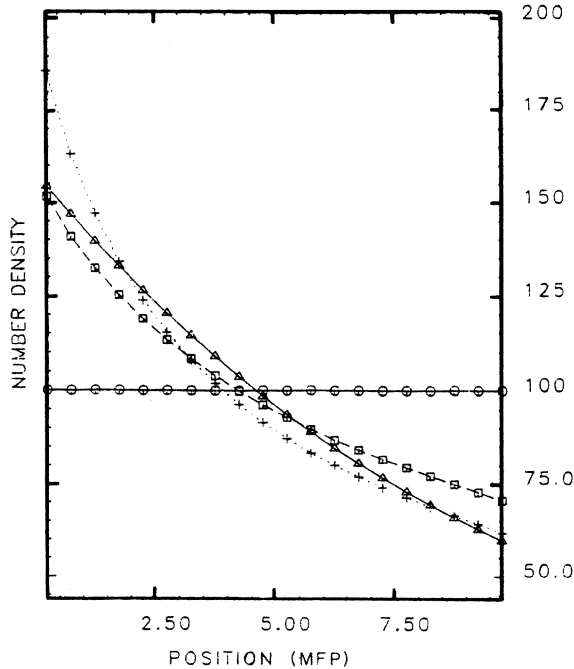


FIG. 1. Plot of number density as a function of cell position. Position is measured in units of mean free path. The solid line with circles is for the equilibrium system ($T_1 = T_2 = 1$) without gravity; the solid line with triangles is for the equilibrium system with gravity. The dashed line with squares is for a temperature gradient of $T_1 = 1, T_2 = 3$. The dotted line with crosses is for a gradient of $T_1 = 1, T_2 = 5$.

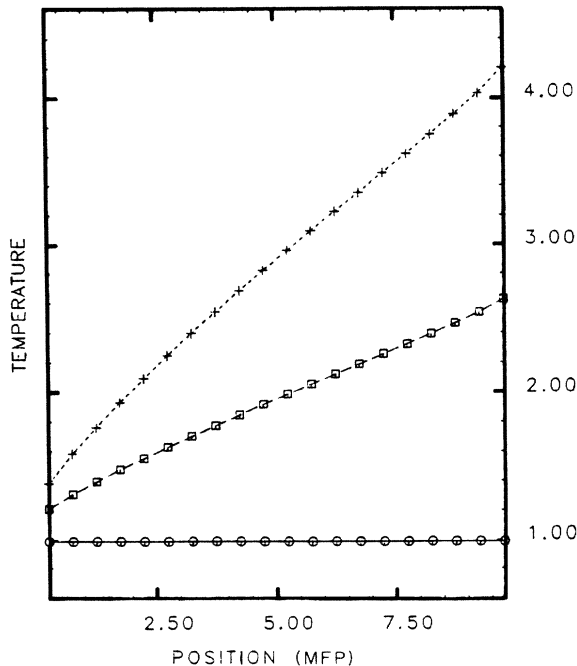


FIG. 2. Plot of temperature as a function of cell position. See Fig. 1 caption. The curves for the equilibrium systems overlap. Note that there is a temperature slip at the wall; as such the gradients are 0.140 and 0.278 degrees per mean free path, respectively.

ber; it vanishes in the thermodynamic limit. Both equilibrium runs (with and without gravity) confirm Eq. (1). Out of equilibrium, the expression is modified to

$$\begin{aligned} \langle \delta n_i \delta n_j \rangle &= n_i \delta_{ij}^{Kr} - \frac{n_i n_j}{\sum_{k=1}^M n_k} + g_{\text{neq}}(\Delta T) \\ &= g_{\text{eq}} + g_{\text{consv}} + g_{\text{neq}}. \end{aligned} \quad (2)$$

Note that we have separated the equilibrium, conservation, and nonequilibrium terms. In Fig. 3 we plot $\langle \delta n_i \delta n_j \rangle - g_{\text{eq}}$ which is also $g_{\text{consv}} + g_{\text{neq}}$ and in Fig. 4 we plot g_{neq} explicitly. The conservation term g_{consv} dominates the nonequilibrium term g_{neq} in our system. A multinomial form for g_{consv} was also found in the free-particle transport problem⁶ and in the self-diffusion problem.⁷ Although according to Fig. 4 the function g_{neq} appears to be nonzero, the statistics are not sufficient to determine either its form or its dependence on temperature gradient. Fluctuating hydrodynamics calculations for liquids yield that g_{neq} is zero to first order in the temperature gradient.¹

For the density-momentum fluctuations the equilibrium and conservation terms are both zero at equilibrium. This is confirmed by both equilibrium runs. Fluctuating hydrodynamics calculations for liquids tell us that the nonequilibrium term should be proportional to the temperature gradient. Furthermore, the spatial dependence should be long ranged as

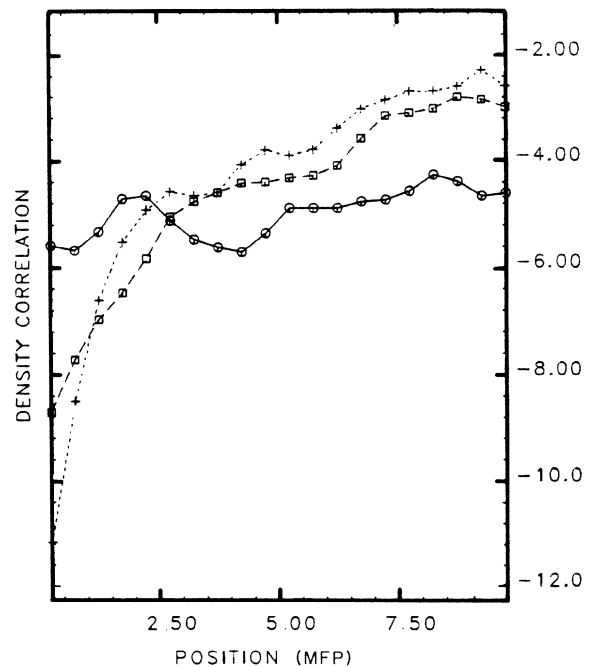


FIG. 3. The function plotted is $\delta n_i \delta n_{11} - n_{11} \delta_{i,11}^{Kr}$, the correlation function for cell 11 with the equilibrium part removed. The function is plotted against the position of cell i . Cell 11 is approximately in the center of the system. See Fig. 1 caption. For clarity, the curve for the equilibrium system with gravity is suppressed; its results confirm (1). The data was smoothed by a (0.25, 0.5, 0.25) filter.

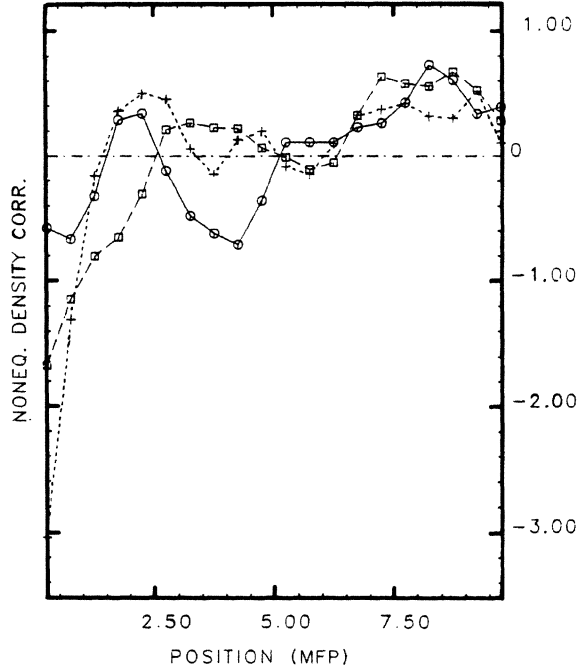


FIG. 4. The function g_{neq} for cell 11. The data was smoothed by a (0.25, 0.5, 0.25) filter. For clarity, the curve for the equilibrium system with gravity is suppressed. The results are comparable for the two equilibrium systems. The reduced correlation function for g_{neq} was also computed [see Eq. (6)] but is not presented here. In no way have I been able to determine the precise functional form of g_{neq} .

$$\langle \delta n_i \delta J_j \rangle \sim \Delta T \times \begin{cases} i(M-j), & i < j \\ j(M-i), & i > j \end{cases} \quad (3)$$

The spatial dependence is linear as opposed to $1/|\mathbf{r}-\mathbf{r}'|$ because we have periodic boundary conditions in the directions perpendicular to the gradient.^{1(f)} The simulation results for the various temperature gradients appear in Fig. 5. We find that the dependence on the gradient is indeed linear but the spatial dependence is modified by the condition of conservation of particle number. This is easily understood if one recalls that $\langle \delta n_i \delta J_j \rangle$ must be zero if we sum over i .

The temperature-temperature correlation function has the form

$$\langle \delta T_i \delta T_j \rangle = \frac{T_i^2}{3/2n_i} \delta_{ij}^{Kr} + g_{\text{neq}}(\Delta T). \quad (4)$$

For high Prandtl number liquids, fluctuating hydrodynamics^{1(e),1(f)} tells us that g_{neq} is quadratic in the temperature gradient and long ranged as

$$g_{\text{neq}}(i,j) \sim (\Delta T)^2 \times \begin{cases} i(M-j), & i < j \\ j(M-i), & i > j \end{cases} \quad (5)$$

One may introduce a reduced correlation function, defined as

$$C(k) \equiv \frac{1}{M-k} \sum_{i=1}^M \sum_{j=i}^M g_{\text{neq}}(i,j) \delta_{i-j,k}^{Kr}. \quad (6)$$

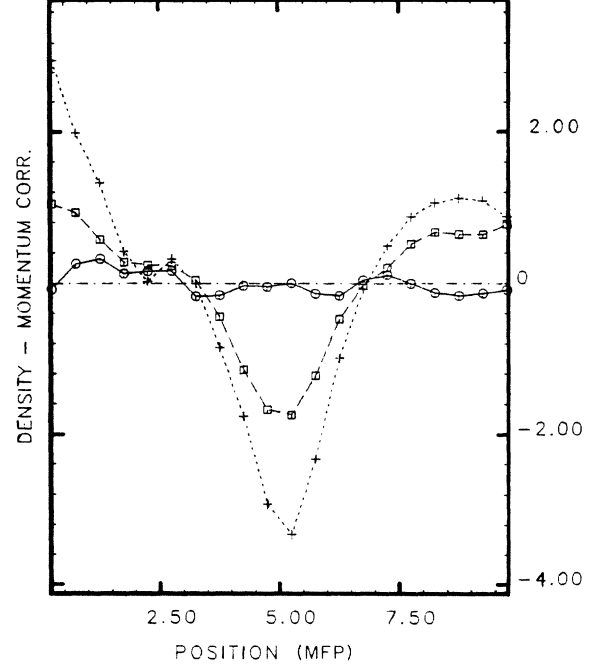


FIG. 5. The number-momentum correlation function for cell 11, $\langle \delta n_i \delta J_{11} \rangle$, plotted as a function of cell position of cell i . For clarity, the curve for the equilibrium system with gravity is suppressed. The results are comparable for the two equilibrium systems. The data is smoothed by a (0.25, 0.5, 0.25) filter. Before filtering, the peak values were 0.299 ($T_1=T_2=1$), -2.18 ($T_1=1, T_2=3$), -3.98 ($T_1=1, T_2=5$).

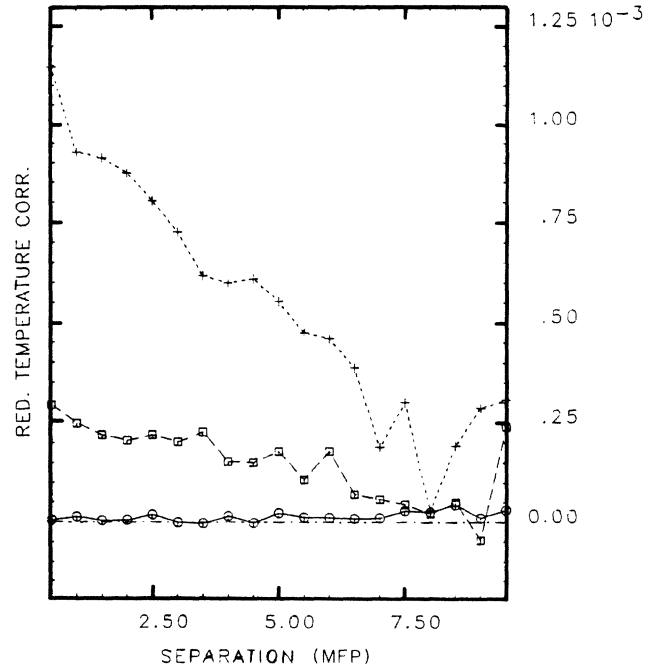


FIG. 6. The reduced-temperature correlation function plotted vs cell separation (in mean free paths). For clarity, the curve for the equilibrium system with gravity is suppressed. The results are comparable for the two equilibrium systems. The values are unsmoothed. Note that the value $C(0)$ is suppressed as it is an order of magnitude larger than the rest of the function.

From (5) we expect that $C(k)$ will be of the form

$$C(k) \sim (\Delta T)^2 (M - k)^2 \quad (7)$$

for large M ; i.e., in the continuous limit ($\sum \rightarrow \int$) of (5) and (6). Because of the quadratic dependence on the gradient, it is difficult to measure $g_{\text{neq}}(i, j)$ directly from the simulation output. The reduced correlation function allows us to average together more data and in effect improve our statistics. Because $g_{\text{neq}}(i, j) \neq g_{\text{neq}}(|i - j|)$, however, the function $C(k)$ is only interesting for this reason. Note that in Fig. 2 of Ref. 3(a), the function plotted is also $C(k)$. In Fig. 6 we plot the reduced correlation function for the various gradients considered. The results are good except that we have suppressed the point $C(0)$ from the curve as it appears to be about 1 order of magnitude too large. The quadratic dependence on temperature gradient appears to be well confirmed as well as the positivity of $C(k)$. A molecular-dynamics study^{3(a)} of a similar system also found a quadratic temperature dependence but did not find $C(k)$ to be strictly positive. Our results do not confirm the quadratic spatial dependence of $C(k)$,

instead the function appears to be linear. This may however be simply due to the paucity of our statistics. The molecular dynamics results^{3(a)} also indicate a linear spatial dependence for $C(k)$.

In conclusion, numerical simulations form a valuable tool in the study of nonequilibrium fluctuating hydrodynamics as a supplement to laboratory experiments. More specifically, Boltzmann-equation-based simulations are very useful because of their simplicity and great speed. More complex problems involving chemistry are currently under study using these simulations. We are especially interested in the effects of fluctuations on the ignition time of a combustion system.

The author wishes to thank Professor M. Malek-Mansour, Professor G. Nicolis, Professor M. Mareschal, and Dr. F. Baras for many valuable discussions. I also wish to thank Professor I. Prigogine for his help and encouragement towards my coming to Bruxelles and Professor E. Clementi for his invitation to IBM Corporation, Kingston, NY.

¹(a) D. Ronis, I. Procaccia, and I. Oppenheim, *Phys. Rev. A* **19**, 1324 (1979); (b) D. Ronis and S. Putterman, *ibid.* **22**, 773 (1980); (c) A. Tremblay, M. Arai, and E. Siggia, *ibid.* **23**, 1451 (1981); (d) T. Kirkpatrick, E. Cohen, and J. Dorfmann, *ibid.* **26**, 972 (1982); (e) G. Nicolis and M. Malek-Mansour, *ibid.* **29**, 2845 (1984); (f) M. Mareschal, in *Non-equilibrium Dynamics in Chemical Systems*, edited by C. Vidal and A. Pacault (Springer-Verlag, Berlin, 1984).

²(a) D. Beysens, Y. Garrabos, and G. Zalczner, *Phys. Rev. Lett.* **45**, 403 (1980); (b) G. Wegdam, N. Keulen, and J. Michielsen,

ibid. **55**, 630 (1985).

³(a) M. Mareschal and E. Kestemont, *Phys. Rev. A* **30**, 1158 (1984); (b) A. Garcia and J. Turner, *Physica A* (to be published).

⁴G. Bird, *Molecular Gas Dynamics* (Clarendon, Oxford, 1976).

⁵A. Garcia, Ph.D. thesis, The University of Texas at Austin, 1984.

⁶A. Garcia (unpublished).

⁷C. Van Den Broeck, W. Horsthemke, and M. Malek-Mansour, *Physica* **89A**, 339 (1977).